Jurnal Nasional Teknik Elektro dan Teknologi Informasi
Volume 13 Number 3 August 2024

Translation of article 10.22146/jnteti.v13i3.9422

GSA With Factor Screening for Performance Evaluation of Transmission Line Protection Relays

Nanang Rohadi[1], Bambang Mukti Wibawa[1], Nendi Suhendi[1]

[1] Department of Electrical Engineering, Faculty of Mathematics and Natural Sciences, Universitas Padjadjaran, Sumedang, Jawa Barat 45364, Indonesia

[Submitted: 6 October 2023, Revised: 6 January 2024, Accepted: 2 June 2024]
Corresponding Author: Nanang Rohadi (email: nanang.rohadi@unpad.ac.id)

ABSTRACT — This paper presents a global sensitivity analysis with factor screening to efficiently test conventional distance relay algorithm models used as transmission line protection devices with series compensators. Various system indeterminacy parameters (factors) may affect the functional performance of the fault impedance measurement algorithm model of intelligent electronic devices, specifically the SEL-421 type distance relays. The purpose of global sensitivity testing is to determine the influence strength of individual and interacting factors on the output of the fault impedance measurement algorithm. Global sensitivity analysis, conducted through variance analysis using quasi-Monte Carlo methods, aims to compute the error in fault impedance measurement results. As an initial step, the Morris method was employed to filter out factors that did not predominantly affect relay performance, thereby reducing the computational burden of the global sensitivity analysis. Several simulated transmission line faults with series compensators and multiple factors were modeled using DIgSILENT PowerFactory. Automatic fault simulations, both before and after compensators, were developed using DIgSILENT Programming Language. The sensitivity of the relay algorithm output was tested for each simulation based on read-out voltage, fault current signals, and the values of sampled factors using both Morris and Sobol methods. The variance of the algorithm output model influenced by several factors was calculated using SIMLAB software. Fault resistance emerged as the dominant factor affecting algorithm performance, with sensitivity indices exceeding 0.9 and 0.7 for faults before and after the compensator, respectively. This technique has effectively tested the SEL-421 distance relay algorithm.

KEYWORDS — Relay Performance, Intelligent Electronic Devices, Global Sensitivity Analysis, Morris Method, DIgSILENT Program Language.

I. INTRODUCTION

Transmission lines with series compensators are often considered as alternatives due to their increased electrical power delivery and efficiency [1]. The network's structure significantly influences the performance of the non-pilot digital distance relay installed to protect the transmission line during a fault [1], [2]. Figure 1 shows the equivalent circuit of a power system with a series compensator placed in the center of the protected line. When a fault occurs after the compensator (CVT+MOV), the fault current read by the relay through the current transformer (CT) affects the fault impedance measurement at the relay point, potentially resulting in relay maloperation, such as overreaching or underreaching [1], [3], [4]. Additionally, uncertain and unknown values of system parameters, i.e, R_F ground fault resistance, δ_F source voltage angle at fault, k_0 zero sequence current compensation, and Z_L line impedance introduces further errors in impedance measurement and fault location determination. These factors cause relay operation faults when the fault occurs before the compensator, and the situation worsens for faults occurring after the compensator [3]. The limitations of using conventional distance relays (such as the SEL-421 distance relay) for line protection with series compensators have been investigated previously [3], [5], [6]. However, a systematic approach to testing the sensitivity of the algorithm, using statistical calculations to assess the influence of various factors, has not been undertaken in previous studies.

The single-phase ground fault shown in Figure 1 is either in the M-O segment before the compensator (fault location at F_1) or in the second O-N segment after the compensator (fault location at F_2). Various indeterminacy parameters (factors) affecting the fault location are shown in red. Several factors influence the performance of the fault impedance measurement by the relay (SEL-421 distance relay) [3]. In the observed case, sensitivity analysis was attempted to be used to assess the influence of such factors on the performance of the relay measurement algorithm. A global sensitivity analysis (GSA) method based on the estimated value of the variance of the algorithm output (error variance) through a quasi-Monte Carlo (QMC) sampling in multidimensional factor space is presented in this paper. This method, originally proposed by Sobol [7], was implemented through SIMLAB software [8]. GSA is a computational process that requires a large number of samples for numerous factors. To expedite the computation, it is recommended to implement a preprocessing stage to reduce the dimensionality of the factor space. Therefore, in this study, Morris' method [9] was implemented to identify the factors that had no effect before applying GSA. This study requires a mathematical model of a transmission line with compensators under fault conditions and a closed-loop impedance fault measurement element, as implemented in an intelligent electronic device (IED), as shown in Figure 1. The SEL-421 distance relay multifunction IED model [10] was implemented using DIgSILENT PowerFactory software [11]. The GSA implementation includes a step to automatically vary the factor values in the transmission line model and run simulations for each fault scenario. Program scripts developed using DIgSILENT Program Language (DPL) are employed for automation functions in fault simulation. Additional scripts are created to calculate the performance index for each fault

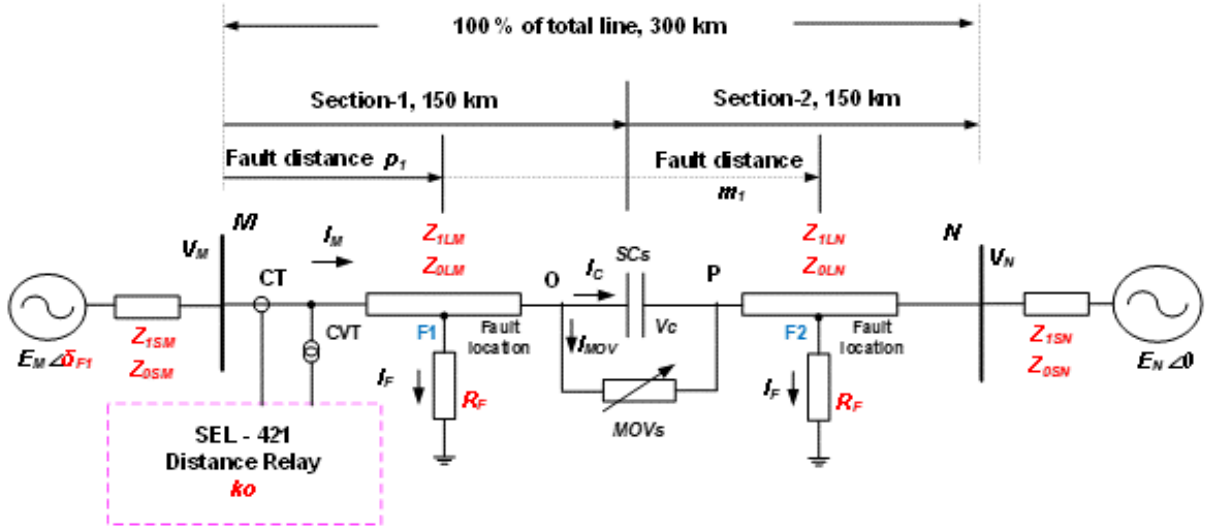

Figure 1. Single transmission line with series compensator: F_1-fault before $SC_S + MOV_S$ dan F_2-fault after $SC_S + MOV_S$.

scenario. By systematically analyzing the effects of multiple factors and as part of protection testing, the proposed technique aids in selecting the optimal IED for a specific line security task when various factors affecting relay performance are considered. The developed testing technique is also useful for manufacturers in the development of protection equipment.

II. FACTOR SPACE AND PERFORMANCE OF FAULT IMPEDANCE MEASUREMENT ALGORITHM

The transmission line model with the series compensator located in the middle of the protected line and the fault location is shown in Figure 1. All elements in the figure were modeled in the DIgSILENT PowerFactory software. The proposed model was used to determine the performance of the distance relay for a phase-A-to-ground fault under various fault scenarios, specifically fault points before and after the compensator (F_1 and F_2) and through the R_F fault resistance. The model includes a set of factors highlighted in red in Figure 1. The performance index values calculated by the SEL-421 impedance measurement algorithm depend on the voltage and current signals resulting from the fault scenarios.

The external system was modeled using a Thevenin equivalent circuit with two voltage sources, E_M and E_N, and positive sequence source impedances, Z_{1SM} and Z_{1SN}, respectively (Figure 1). During the simulation of the phase-A-to-ground fault, the fault impedances (1) and (8) were calculated by the relay based on the zero-sequence current compensation method, I_0, using the k_0 correction factor [3], [12]. The k_0 factor in (3) depended on the Z_{0L} zero-sequence line impedance which was not precisely known. For faults on segment-2 (between P and N in Figure 1), the fault impedance calculation could become more complex due to the presence of compensators affecting the fault impedance calculation [2], [3], [13]. For fault location in segment-1, the Z_m fault impedance in (1) measured from the relay location to the F_1 fault point (p_1 distance in Figure 1) is not always the actual fault impedance, i.e., $p_1 Z_{1LM}$. The fault impedance, Z_m (Ω), estimated by the relay algorithm is derived as follows [3].

$$Z_m(before) = \frac{V_{AM}}{I^c_{AM}} = p_1 Z_{1LM} + \Delta Z_{1(F1)} \quad (1)$$

given V_{AM} (V) represents the phase-A voltage and I^c_{AM} (A) denotes the I_{AM} current measured from phase-A current through the secondary of the current transformer (CT), compensated by the I_{0AM} zero sequence current , which is also measured by the relay algorithm. The compensated phase-A current measurement is further expressed by (2).

$$I^c_{AM} = I_{AM} + k_0 I_{0AM}. \quad (2)$$

The k_0 zero-sequence compensation factor is further expressed by (3) [12].

$$k_0 = \frac{Z_{0L} - Z_{1L}}{Z_{1L}}. \quad (3)$$

It is observable that in the calculation of the impedance measurement in (1) for a single-phase to ground fault, Z_m, there is a fault impedance measurement error of $\Delta Z_1(\Omega)$, which is influenced by several factors. The zero-sequence compensation factor, k_0, in (3) needs to be corrected to avoid errors in fault impedance calculation when a phase-to-ground fault occurs [12]. This positive sequence impedance error, denoted by ΔZ_1, is an f_1 nonlinear function of several factors, namely the $\boldsymbol{P_L}, \boldsymbol{P_S}, \boldsymbol{P_E}$, parameter vectors, the R_F fault resistance, the p_1 fault distance, and the δ_F load flow angle, as stated in (4).

$$\Delta Z_{1(F1)} = f_1(\boldsymbol{P_E}, \boldsymbol{P_S}, \boldsymbol{P_L}, R_F, p_1) \quad (4)$$

given

$\boldsymbol{P_L} = [Z_{1LM}, Z_{1LN}, Z_{0LM}, Z_{0LN}]^T$,

$\boldsymbol{P_S} = [Z_{1SM}, Z_{1SN}, Z_{0SM}, Z_{0SN}]^T$,

$\boldsymbol{P_E} = [E_M \angle\delta_{F1}, E_N \angle\delta_{F2}]^T$; $\delta_{F2} = 0$.

The fault impedance calculation became more complex for faults occurring after the compensator fault (fault at F_2). To address this, a sequence of symmetrical components was used for the impedance calculation.

Specifically, for a phase-A-to-ground fault after the compensator (fault at F_2), the calculation is explained using symmetrical components. The symmetrical voltage sequence, incorporating the R_F fault resistance factor, is expressed by (5) [3], [14].

$$\underline{V_1} + \underline{V_2} + \underline{V_0} = 3R_F \underline{I_F}. \quad (5)$$

Furthermore, the symmetrical stress in (5) is expressed as shown in (6).

TABLE I
SYSTEM DATA

Transmission Line (P_L)		
Length of transmission line	km	300
Compensation level (C)	%	70
Fault location	p.u	0.4, 0.6, 0.8, 1
Positive sequence impedance	Ω	8.4+*j*94.5
Zero sequence impedance	Ω	82.5+*j*308.1
Positive sequence capacitance	nF/km	4.7
Zero sequence capacitance	nF/km	9.67
MOVs (Figure 1)		
Current reference	kA	1
Voltage reference	kV	150
Exponent	-	23
System M (P_S)		
Positive sequence impedance	Ω	0.656+*j*7.5
Zero sequence impedance	Ω	1.167+*j*11.25
System N (P_S)		
Positive sequence impedance	Ω	1.31+*j*15
Zero sequence impedance	Ω	2.33+*j*26.6
Sources (P_E)		
System frequency	Hz	50
System voltage (E_M)	kV	$230\angle\delta_{F1}°$
System voltage (E_N)	kV	$230\angle\delta_{F2}°$

$$\begin{aligned} V_1 &= V_{1AM} - Z_{1LM}I_{1AM} - V_{1C} - mZ_{1LN}I_{1AN} \\ V_2 &= V_{2AM} - Z_{2LM}I_{2AM} - V_{2C} - mZ_{2LN}I_{2AN} \\ V_0 &= V_{0AM} - Z_{0LM}I_{0AM} - V_{0C} - mZ_{0LN}I_{0AN} \end{aligned} \quad (6)$$

given m is the P-N segment, representing the distance from the capacitor to the F_2 fault point; V_C is the voltage drop at *SCs+MOVs*, and $V_{1,2,0}$ are the positive, negative and zero sequence voltages, respectively.

The positive sequence line is expressed similarly to the negative sequence impedance, i.e., $Z_{1L} = Z_{2L}$. Then, the phase voltage measurement is described as in (7).

$$\begin{aligned} V_{AM} &= V_C + Z_{1LM}\left[I_{AM} + \frac{Z_{0LM} - Z_{1LM}}{Z_{1LM}} I_{0AM}\right] + 3R_F I_F \\ V_{AM} &= V_C + Z_{1LM}[I_{AM} + k_0 I_{0AM}] + 3R_F I_F \\ V_{AM} &= V_C + Z_{1LM} I_{AM}^C + 3R_F I_F \end{aligned} \quad (7)$$

given

$V_{AM} = V_{1AM} + V_{2AM} + V_{0AM}$

$V_C = V_{1C} + V_{2C} + V_{0C}$

$I_{AM} = I_{1AM} + I_{2AM} + I_{0AM}$

$Z_{1LMN} = Z_{1LM} + mZ_{1LN}$

$Z_{2LMN} = Z_{2LM} + mZ_{2LN}$

$Z_{0LMN} = Z_{0LM} + mZ_{0LN}$

so that the impedance measurement at the F_2 fault point is expressed by (8).

$$\begin{aligned} Z_m(after) &= \frac{V_{AM}}{I_{AM}^C} = Z_{1LMN} + 3R_F \frac{I_F}{I_{AM}^C} + \frac{V_C}{I_{AM}^C} \\ &= Z_{1LMN} + \Delta Z_{1(F2)} \end{aligned} \quad (8)$$

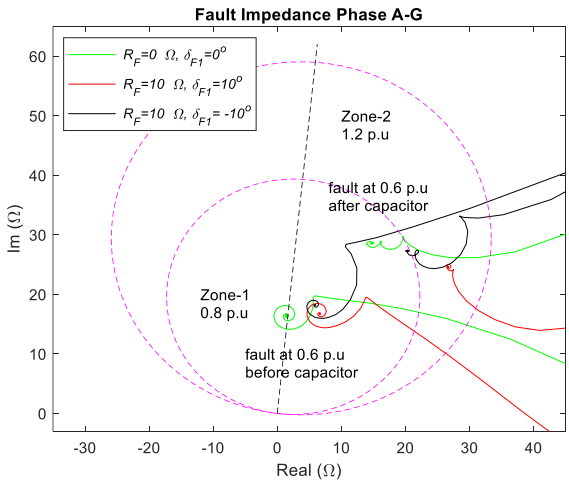

Figure 2. Influence of fault resistance (R_F) and dan load flow angel (δ_F) on Z_{1m} fault impedance measurement before and after compensator.

where V_{AM} is the phase voltage A to ground measured by the relay on the M side, and I_{MA}^C denotes the I_{AM} phase current that has been compensated with the I_0 zero-sequence current, as described in (2). The k_0 zero-sequence compensation factor in (2) is defined in the (3). Additionally, from the measurement in (8), the measurement error is expressed as shown in (9).

$$\Delta Z_{1(F2)} = f_2\left(\boldsymbol{P_E}, \boldsymbol{P_S}, \boldsymbol{P_L}, R_F, p_2, C\right) = f_2(\boldsymbol{x}_i), \;\; i = 1,..,n \quad (9)$$

where $\boldsymbol{x}$ is a vector of n factors, p_2 represents the fault location distance, and C denotes the series compensator.

Several simulation experiments were conducted to assess the influence of various factors on the fault impedance measurement error by the relay. The utilized circuit model is shown in Figure 1, with the parameter values for the simulation experiments presented in Table I.

The distance relay protection range for the Zone-1 area was set to 0.8 p.u of the total positive sequence impedance of the line, which included the length of segment-1 (M-O in Figure 1) plus the length of lines after the compensator (segment-2, P-N). The line was homogenized so that the line impedance per unit length for both segments was identical. Figure 2 demonstrates the fault impedance measurement results for a simulated single-phase A to ground fault at point 0.6 p.u before and after the compensator. In addition, Figure 2 also shows that fault impedance measurement error, which is directly proportional to the distance to the fault point, is influenced by several factors, such as the ground fault resistance, R_F, and load flow angle, δ_F. It is evident that the impact of ground failure resistance on impedance measurement is significant, depending on the failure resistance. Similarly, this effect is noticeable when combined with the load flow angle. Due to the influence of ground resistance, the measurement results are shifted to the right. Additionally, the impact of the load flow angle causes the impedance value to shift up or down, as shown in Figure 2 in black and red. The worst condition of impedance measurement is interference after the compensator, which may lead to the relay overreaching, as illustrated in Figure 2.

Under real conditions, certain system parameters are often uncertain (as shown in Figure 1 in red). Therefore, a range of parameter values, as shown in Table II, was assumed for the $\boldsymbol{P_E}, \boldsymbol{P_S}, \boldsymbol{P_L}, R_F, \delta_F, k_o$ parameters (several factors) that might cause errors in the fault impedance measurement. This study assumed a total of 19 factors, each with a uniform variation of

TABLE II
FACTOR SPECIFICATIONS

Indeterminacy Parameter x_i	Description x_i	Interval variation
x_1	R_F	[0 ; 10 Ω]
x_2	δ_{F1}	[-10 ; 10]
x_3	k_o	[0.714 ; 0.873]
x_4	$Re\{Z_{1SM}\}$	[0.590 ; 0.721 Ω]
x_5	$Im\{Z_{1SM}\}$	[6.75 ; 8.25 Ω]
x_6	$Re\{Z_{0SM}\}$	[1.05 ; 1.28 Ω]
x_7	$Im\{Z_{0SM}\}$	[10.125 ; 12.375 Ω]
x_8	$Re\{Z_{1SN}\}$	[1.18 ; 1.44 Ω]
x_9	$Im\{Z_{1SN}\}$	[13.5 ; 16.5 Ω]
x_{10}	$Re\{Z_{0SN}\}$	[2.09 ; 2.56 Ω]
x_{11}	$Im\{Z_{0SN}\}$	[23.94 ; 29.26 Ω]
x_{12}	$Re\{Z_{1LM}\}$	[0.025 ; 0.030 Ω]
x_{13}	$Im\{Z_{1LM}\}$	[0.283 ; 0.346 Ω]
x_{14}	$Re\{Z_{0LM}\}$	[0.247 ; 0.302 Ω]
x_{15}	$Im\{Z_{0LM}\}$	[0.924 ; 1.129 Ω]
x_{16}	$Re\{Z_{1LN}\}$	[0.025 ; 0.031 Ω]
x_{17}	$Im\{Z_{1LN}\}$	[0.283 ; 0.346 Ω]
x_{18}	$Re\{Z_{0LN}\}$	[0.247 ; 0.302 Ω]
x_{19}	$Im\{Z_{0LN}\}$	[0.924 ; 1.129 Ω]

10%. These factors were described as having high multidimensionality within the data space. To illustrate the factor influence, several fault experiment scenarios were conducted for both before and after the compensator, with parameter values adjusted according to the created data samples. Each fault simulation simultaneously read the changes in each $\boldsymbol{x}_i \in S$ random variable vector, from S sample through the developed algorithm. The algorithm developed for simulating the SEL-421 distance relay model read each value of the sample vector as a factor and calculates the fault impedance for each simulation. The impedance calculation results are marked with '*' and '+', representing the function of the $\boldsymbol{y}_i = f(\boldsymbol{x}_i)$ sample vector, as shown in Figure 3.

Several factors with random values affected the performance of the relay algorithm observed for two fault locations: a fault before the compensator on segment-1 and fault after the compensator on segment-2. Figure 3 illustrates the $\boldsymbol{x}_i$ indeterminacy factor on the accuracy of the fault impedance calculation algorithm, manifested as $\boldsymbol{y}_i$ output indeterminacy. It was further observed that various factors affecting relay performance and impedance calculation errors were going to be introduced due to the compensator. A fault in segment-2 resulted in a measurement that placed fault location in Zone-2 for all fault positions at 0.4, 0.6, and 0.8 p.u after the compensator. This might lead to relay maloperation in the form of underreach or overreach in distance relays. This issue is explained by a systematic fault impedance measurement error or a deviation in the measurement results caused by the influence of an $\boldsymbol{x}_i$ single factor, or the interaction between factors $\boldsymbol{x}_i$ .. $\boldsymbol{x}_n$. Weaknesses in relay performance due to various influencing factors are mitigated by improving the impedance calculation algorithm on the relay (i.e., impedance calculation while ignoring its influencing factors). This research solely explored these issues through systematic testing, specifically by observing the influence of these factors on the algorithm's performance.

The algorithm performance was observed through quantifying the $y_{i(error)}$ (10) output error as a function of the

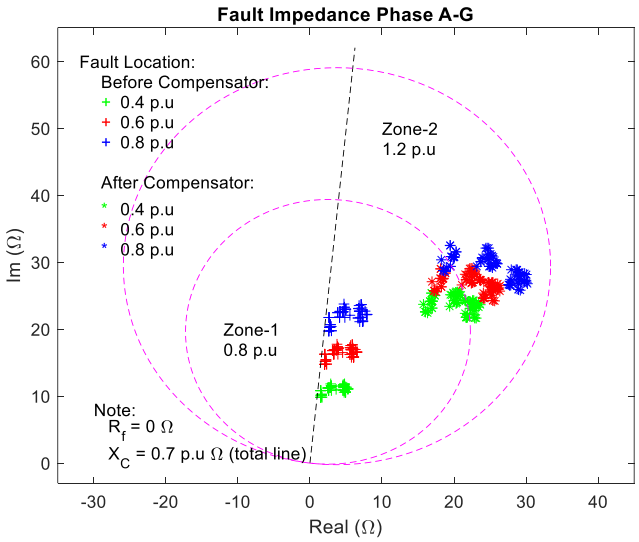

Figure 3. Influence of a number of factors (Figure 1) on fault impedance measurements before and after compensators.

$\boldsymbol{x}_i$ factor vector. The technique developed for analyzing the algorithm's sensitivity to factors was based on error variance analysis of the expected error of several $\boldsymbol{x}_i = \mathbb{R}^n$ samples where n is the sample dimension. The value of n = 19 factor dimension was quite large for the observed case. Therefore, it took a very high computational time when the variance analysis approach using Sobol's technique was performed. In this case, a factor screening method needed to be performed to increase the computational efficiency of the analysis of variance. The factor screening technique using the Morris method was intended to eliminate factors considered unnecessary before the Sobol technique for measurement error variance analysis was performed. This sensitivity analysis technique employed the sampling technique, making it possible to estimate the sensitivity of the impedance error of the measurement results caused by several factors, both individually and due to the interaction between two or more factors.

III. SENSITIVITY ANALYSIS OF FAULT IMPEDANCE MEASUREMENT ALGORITHM

The impact of a single factor and the interaction of multiple factors were evaluated based on the fault impedance error value in (10) derived from the measurement results by the relay algorithm for each ith simulation. The performance index of the measurement error was calculated as the absolute difference between the actual impedance measurement result, y_i, and the expected value, $E[y_i]$, as follows:

$$y_{i(error)} = |y_i - E[y_i]|\ \Omega. \quad (10)$$

The impedance error measurement, as the relay algorithm output, is a nonlinear function of several factors and is expressed as $y_i = f(\boldsymbol{x_i})$, as described in (1) and (8). The number of factors used and stored in $\boldsymbol{x} = \mathbb{R}^n$ factor (where $\mathbb{R}$ is the set of real numbers with n factor dimension) is shown in Table II. For the data-sampling-based fault simulation, all factors $\boldsymbol{x}_i$ were continuously varied based on a sequence of quasi-random data generated over a predetermined range of uniformly distributed intervals. Using the quasi-random technique with several n factors generated a relatively large Ω data universe. Consequently, significant computational time was required to meet the GSA requirement for measurement error, as referenced in (10).

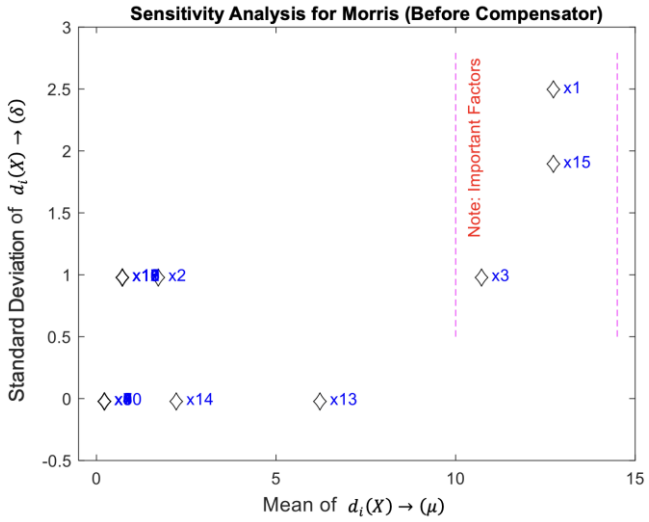

(a)

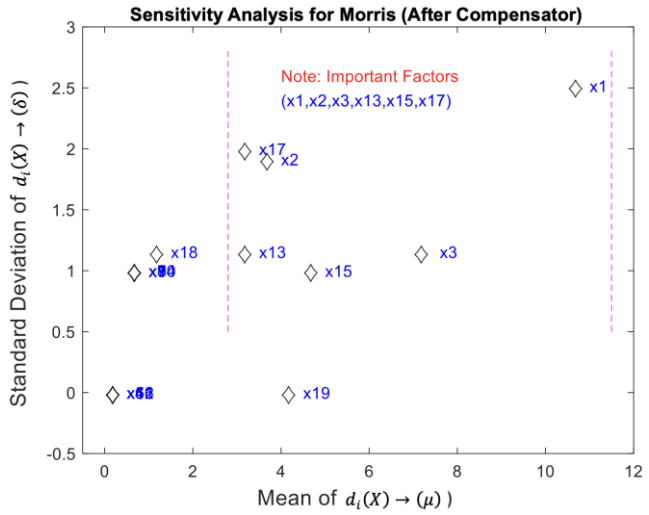

(b)

Figure 4. Local sensitivity with Morris method, (a) before compensator, (b) after compensator.

A. LOCAL SENSITIVITY ANALYSIS

The classical approach to relay sensitivity analysis, as seen in previous research, requires only a small number of samples, examining the influence of one factor while holding others constant. This technique is primarily used to rank the factors affecting relay performance but does not consider the overall concurrent uncertainty of these factors or analyze their sensitivity comprehensively. Therefore, in this study, a combined technique involving both local and global analysis approaches was employed for accurate and efficient sensitivity analysis [15]. Local sensitivity analysis using the Morris method was conducted to measure the influence of individual factors on relay performance (see Figure 4). Screening various factors through the Morris method identifies their individual influence levels on relay performance, allowing the subsequent global sensitivity analysis using the Sobol technique and quasi-random samples to require a smaller sample size.

In this study, the Morris method was utilized for local sensitivity analysis. This method is simple yet effective for screening input factors that may affect the characteristics of relay algorithm models [9], [16]. The technique employs a uniquely randomized scheme of varying a single factor at a time. The evaluation index of the Morris method is called the one-factor effect, which measures the effect of the ith factor by performing computations exclusively with that factor. Considering that the computational model of the relay algorithm was affected by several input factors as shown in red (Figure 1) and expressed by x, $i = 1,2,\dots,n$, the variation of N_s values of the $\boldsymbol{x}$ random factor over the unit interval [0.1] was at $(p-1)$ partition level with p (an even number) being the specified level, and $N_s \in \Omega$. For a given factor vector value at each $\boldsymbol{x}$ simulation, the influence of the ith factor on the model was defined by (11) [9].

$$d_i(\boldsymbol{x}) = \frac{[y(x_1,\dots,x_{i-1},x_i+\Delta,x_{i+1},\dots,x_k)-y(x)]}{\Delta}. \quad (11)$$

The value of Δ is determined from the $\{1/(p-1),\dots 1-1/(p-1)\}$ data set. The value of $\boldsymbol{x} = (x_1, x_2, \dots x_n)$ is determined in the Ω data universe such that, from (10), the value of $\boldsymbol{x_i}$ transforms to $(\boldsymbol{x_i} + \boldsymbol{e_i}\Delta) \in \Omega$. The value of $\boldsymbol{e}_i$ is a zero-vector adapted according to the ith data sample. Based on the above explanation, the value distribution pattern of F_i is expressed as $d_i(\boldsymbol{x}) \sim F_i$ in (11). The data of the input random variables, i.e., the elements of F_i, are $p^{k-1}[p-\Delta(p-1)]$. The local sensitivity analysis of the impedance measurement algorithms in (1) and (8) is based on the Morris method. The local sensitivity of the fault impedance measurement is determined by mapping the F_i value (value distribution) in the form of the μ mean value to the σ standard deviation value. The degree of influence of factor x_i on the relay impedance measurement algorithm Z_m is determined by calculating the μ and σ values based on the $d_i(\boldsymbol{x}) \sim F_i$ value distribution. The μ value indicates the influence level of a single factor, while the σ value indicates the influence level resulting from the interaction between multiple factors (see Figure 4).

B. GLOBAL SENSITIVITY ANALYSIS

GSA using the QMC technique with quasi-random sampling data was effectively implemented after performing the x-factor screening process with the Morris method, as described above. This approach reduces the factor dimension computed through the Sobol method for GSA. For a small n factor universe dimension, GSA with QMC and quasi-random sampling is the most effective global sensitivity method and achieves fast convergence [15], [17], [18]. The GSA was performed based on the sampling data, with the solution procedure described in Figure 5.

The indeterminacy of the relay algorithm output, which serves as the performance index for impedance calculation, was measured by the variance of the calculation error. To determine the degree of influence of $\boldsymbol{x}$ factor, whether individually or through interactions with other factors, it is necessary to calculate the variance component attributable to the factor. It was achieved by calculating the average of f_i in (12), which is affected by multiple $\boldsymbol{x}$ factors except for the factor under observation. The variance of f_i influenced solely by the individual factor x_i is then described as follows.

$$f_i(x_i) = \int f(x) \prod_{k\neq 1} dx_k - f_0 \quad (12)$$

$$V_i = f_i(x_i)^2 = \int f(x)^2 \prod_{k\neq i} dx_k - {f_0}^2 \quad (13)$$

where V_i is the variance performance index attributed to x_i and is expressed as

$$D_i = \sigma_{X_i}^2\{E\{f(\boldsymbol{x})|x_i\}\} \quad (14)$$

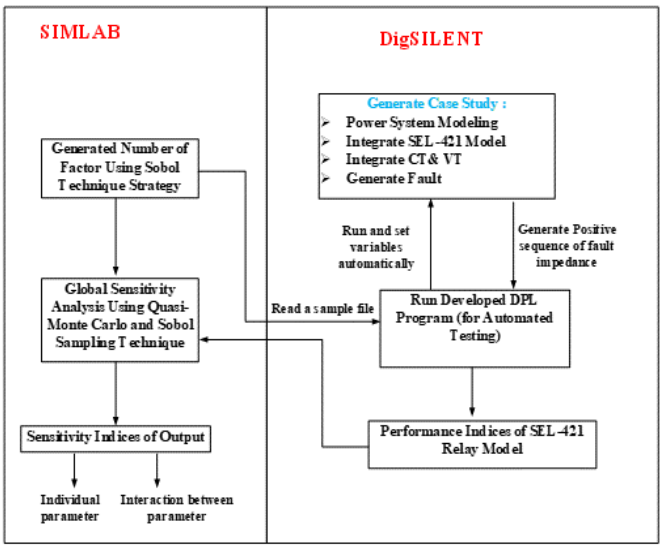

Figure 5. Proposed GSA method.

given $E\{*\}$ is the expected value of the output variance expressed as

$$f_0 = \int f(x)dx. \tag{15}$$

Then, the global sensitivity attributed to the S_i individual factor is expressed by (16).

$$S_i = \frac{\sigma^2_{X_i}\{E\{f(x)|X_i\}\}}{\sigma^2_X\{E\{f(x)\}\}} = \frac{V_i}{\sigma^2\{f(x)\}} \tag{16}$$

where $\sigma^2\{f(\boldsymbol{x})\}$ is the total performance variance of the output index, which is also calculated with the integral through QMC. When the sum of the sensitization probabilities of S_i is not zero, the total sensitization is generated due to the interaction effect between the factors [19]. The V_{ij} variance and D_{ij} sensitivity resulting from the interaction between the two factors, x_i and x_j, is then be defined as in (17) to (19).

$$f_{ij}(x_i, x_j) = \int f(x) \prod_{k\neq i,j} dx_k - f_0 - f_i(x_i) - f_j(x_j) \tag{17}$$

$$D_{ij} = f_{ij}(x_i, x_j)^2 = \int f(x)^2 \prod_{k\neq ij} dx_k - {f_0}^2 - V_i - V_j \tag{18}$$

$$V_{ij} = \sigma^2_{X_{ij}}\left\{E\{f(\boldsymbol{x})|x_i, x_j\}\right\}. \tag{19}$$

Furthermore, the sensitivity index for the interaction between factors is defined by (20).

$$S_{ij} = \frac{\sigma^2_{X_{ij}}\left\{E\{f(x)|x_i,x_j\}\right\}}{\sigma^2_X\{E\{f(x)\}\}} = \frac{V_{ij}}{\sigma^2\{f(x)\}}. \tag{20}$$

It is stated that the analysis of variance using the Sobol technique is based on decomposing the f model into multiple dimensions of subfunctions, as described in (21).

$$\begin{aligned} f(\boldsymbol{X}) &= f_0 + \sum_i f_i(x_i) + \sum_{i<j} f_{ij}(x_i, x_j) + \cdots \\ &\quad + f_{i..d}(x_i, \ldots, x_n) \\ &= f_0 + \textstyle\sum_{\boldsymbol{u}\subset \boldsymbol{D}} f_u(\boldsymbol{x}_u) \end{aligned} \tag{21}$$

given $\boldsymbol{D} = \{1, \ldots, n\}$, , let $\boldsymbol{x}_u$ be the sub vector of $\boldsymbol{x}$, where $\boldsymbol{x}$ represents the random variable and factors expressed by $\boldsymbol{u} = \{i_1, \ldots, i_S\}, S \leq n$ subset. For several indeterminacy parameters (factors), n, the total variance of the index is the sum of the variances of the subsets [20], [21], as shown in (22).

$$\sigma^2\{f(\boldsymbol{X})\} = V_u^T = \textstyle\sum_{i=1}^n V_i + \sum_{i<j} V_{ij} + \cdots + V_{1,2,..,n}. \tag{22}$$

Furthermore, the total sensitivity index is represented as follows:

$$\textstyle\sum_{i=1}^d S_i + \sum_{i<j} S_{ij} + \cdots + S_{1,2,..,d} = 1. \tag{23}$$

The GSA procedure depicted in Figure 5 is utilized to assess the global sensitivity of impedance measurements to various influencing factors. Figure 6 illustrates the results of sensitivity testing for faults both before and after the compensator.

IV. RESULTS AND DISCUSSION

Simulation of phase A to ground faults at various fault locations (Figure 1) was conducted using DIgSILENT PowerFactory software. The variation in the values of several factors, represented as $\boldsymbol{x} = \mathbb{R}^{19}$, was uniformly distributed within a specific range, as shown in Table II. The fault impedance measurement performance of the relay was evaluated for both before and after compensator faults within the data universe of the $\boldsymbol{x}$ factor. This data universe of factors was generated through SIMLAB software, utilizing the Morris method and Sobol's quasi-random sequence. Two sensitivity analysis methods, namely local and global, were also applied using SIMLAB for all statistical calculations and sensitivity measures of the algorithm's output performance index. Local sensitivity, also known as one-at-a-time (OAT), was observed based on changes in a single factor. In contrast, global sensitivities were derived from the entire factor space.

The results of measuring local sensitivity using the Morris method are shown in Figure 4. This technique presents sensitivity results for factor ranking purposes through a mapping between the standard deviation value σ and the mean value (μ) for all effects of the $\boldsymbol{x}_i$ factor. In this study, the results were calculated using the Morris technique with 80 data samples, which is considered sufficient for the number of $\boldsymbol{x}_i$ factors. Figure 4 shows that a large value of μ indicates the dominance of the factor on the relay performance index, while a large value of σ indicates a significant interaction effect between factors. Figure 4(a) shows the simulation results before the compensator, identifying the dominant factors: $x_1\,(R_F)$, $x_{15}\,(imZ_{1LM})$, $x_3(k_o)$. Figure 4(b) displays the simulation results after the compensator, identifying the dominant factors affecting the performance of the relay algorithm, which include $x_1\,(R_F)$, $x_2\,(\delta_{F1})$, $x_3(k_0)$, $x_{13}\,(reZ_{1LM})$, $x_{15}(imZ_{1LM})$, $x_{17}(reZ_{1LM})$, dan $x_{19}(imZ_{1LM})$.

From the results obtained using the Morris method, it is evident that factor x_1 has a significant μ variance, indicating that the performance of the model index, specifically the impedance measurement error value, is influenced by the value of x_1 individually. The σ standard deviation of x_1 is also considerable, suggesting that the interaction of x_1 with other factors significantly affects relay performance. The x_3 factor also has a notable impact after x_1, contributing both individually and through interactions with other factors to the accuracy of the relay performance. Furthermore, Figure 4 presents the analysis of the sensitivity values obtained by the Morris method for a fault location of 0.6 p.u in two segments, i.e., before and after the compensator. Based on this understanding, Figure 1 and Table II assumes seven factors to be dominant in affecting the performance index of the relay algorithm for the 0.6 p.u fault location example: X_1, X_2, X_3, X_{13}, X_{15}, X_{17}, and X_{19}.

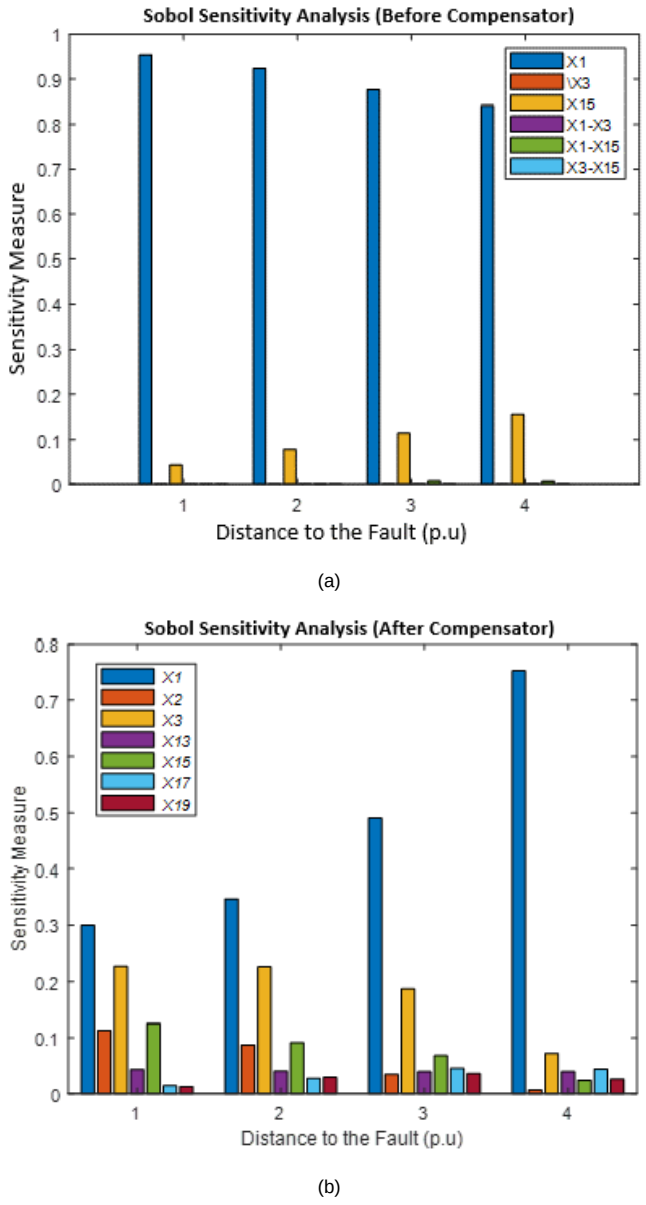

Figure 6. GSA of several factors, (a) global sensitivity to fault before compensator, (b) global sensitivity to fault after compensator.

Local sensitivity using the Morris method was employed to screen the $\boldsymbol{x} = \{x_1, x_2, \ldots, x_{19}\}$, factors reducing them from 19 factors to 3 factors before the compensator and 7 factors after the compensator. This dominant factor screening significantly reduces the computational effort required to assess overall sensitivity with GSA based on quasi-random sampling. The optimal value of the data universe for the seven factors selected by the Morris method was generated through SIMLAB, which was 80 data samples. Furthermore, for GSA analysis, fault simulation with DIgSILENT was used to estimate impedance faults at locations of 0.4 p.u, 0.6 p.u, 0.8 p.u, and 1 p.u of two MN line segments. For each fault simulation, variations in the values of the three and seven factors were performed, with a total of 16,384 and 15,360 data samples based on quasi-random sampling, respectively.

The performance index calculation against the fault impedance measurement function, based on variations in the factor value, was executed by the relay algorithm. Additionally, the procedure for sensitivity index calculation was estimated using SIMLAB (see Figure 5). The results of the estimated sensitivity index calculation, employing the statistical calculation approach, are presented in Figure 6. The conclusions of the global sensitivity analysis, as illustrated in Figure 6, are detailed as follows.

As depicted in Figure 6(a), the x_1 (R_F) factor exhibits a decreasing trend when the fault occurs before the compensator and further from the relay location. Conversely, when the fault occurs after the compensator (Figure 6(b)), the influence of the fault resistance increases. Both scenarios indicate that the influence of the R_F fault resistance remains very dominant for each fault location.

The x_2 (δ_{F1}) factor significantly impacts relay performance following a resistance failure, particularly for faults occurring after the compensator (see Figure 6(b)). The influence of $x_3(k_o)$ also pertains to faults after the compensator, exhibiting a decreasing effect relative to the fault location. Similarly, x_2 (δ_{F1}) shows the same influence (see Figure 6(b)).

For the effect of the interaction factor, the observation focused on the interaction between x_1 and x_{15}. The characteristics resulting from this interaction increase for fault locations after the compensator and decrease for faults at 0.8 p.u and 1 p.u. This behavior is attributed to the installation of a series compensator at 70% of the total channel length.

The developed testing technique is highly effective for evaluating protection relays. This test simulates real-world conditions, allowing all factors to be analyzed simultaneously. Compared to previous methods, this technique enhances test results by enabling the observation of both individual influences and the interactions between factors on relay performance.

V. CONCLUSION

In this paper, a methodology for a systematic sensitivity study of the fault impedance measurement function of the distance relay IED model SEL-421 in the context of a single transmission line with a series compensator is presented. The testing technique was developed through variance analysis of the computational measurement error by an algorithm influenced by several factors. To eliminate less influential factors and reduce the dimension of the factor space, a factor screening method using the Morris method was performed first. For the presented case, the dimension of the factor space was reduced from 19 to 7 factors, followed by a global analysis based on quasi-random sampling of the factor space. From the analysis, it is concluded that the ground failure resistance x_1 (R_F) is a crucial factor to consider. The working accuracy of the relay is significantly influenced by the relay algorithm's ability to mitigate the impact of the dominant R_F factor across all fault locations when calculating fault impedance. Fault impedance is also sensitive to the $x_3(k_0)$ zero-sequence compensator. This value is significantly affected by the uncertainty in the zero-sequence impedance of the line, as well as by the positive sequence impedance, which is inherently influenced by the load flow angle at the time of the fault.

The methodology was implemented in two software environments: DIgSILENT, for system modeling, fault simulation, and fault impedance measurements using the SEL-421 distance relay algorithm; and SIMLAB, for sampling sequences and estimating algorithm sensitivity as a function of uncertainty parameters. The proposed methodology is highly useful for testing various IED performance applications, facilitating comparisons, and identifying factors that influence

relay settings and backup strategies. This testing technique benefits both relay users and manufacturers, aiding in the use and development of relays when uncertainty factors need to be considered.

CONFLICTS OF INTEREST

The authors declare that they have no conflicts of interest related to this publication.

AUTHORS' CONTRIBUTIONS

Conceptualization, Nanang Rohadi; methodology, Nanang Rohadi; software, Nanang Rohadi; validation, Nanang Rohadi; formal analysis, Nanang Rohadi; visualization, Nanang Rohadi; project administration, Bambang Mukti Wibawa and Nendi Suhendi; editing, Bambang Mukti Wibawa and Nendi Suhendi.

ACKNOWLEDGMENT

The authors gratefully acknowledge the financial support from Universitas Padjadjaran and the Faculty of Mathematics and Natural Sciences, which made this research possible.

REFERENCES

[1] A. Purohit and V. Gohokar, "Maloperation of distance relay under faulty conditions in presence of static synchronous series compensator," *2019 IEEE 2nd Int. Conf. Power Energy Appl. (ICPEA)*, 2019, pp. 66–70, doi: 10.1109/ICPEA.2019.8818520.

[2] D.K. Ibrahim, G.M. Abo-Hamad, E.E.-D.M.A. Zahab, and A.F. Zobaa, "Comprehensive analysis of the impact of the TCSC on distance relays in interconnected transmission networks," *IEEE Access*, vol. 8, pp. 228315–228325, Dec. 2020, doi: 10.1109/ACCESS.2020.3046532.

[3] N. Rohadi and N. Suhendi, "Investigasi kinerja relai proteksi saluran transmisi dengan kompensator seri," *J. Nas. Tek. Elekt. Teknol. Inf.*, vol 12, no.3, pp. 190–196, Aug. 2023, doi: 10.22146/jnteti.v12i3.4810.

[4] A. Kalita, "Overreaching of reactive reach in distance protection relay for faults involving earth path and soil resistivity as a limiting determinant," *2022 22nd Nat. Power Syst. Conf. (NPSC)*, 2022, pp. 385–389, doi: 10.1109/NPSC57038.2022.10069392.

[5] N. Rohadi, N. Suhendi, and L.K. Men, "Teknik pengujian kinerja algoritma relay jarak menggunakan DIgSILENT," *J. Nas. Tek. Elekt. Teknol. Inf.*, vol 10, no. 1, pp. 85–90, Feb. 2021, doi: 10.22146/jnteti.v10i1.735.

[6] Y. Liang *et al.*, "A novel fault impedance calculation method for distance protection against fault resistance," *IEEE Trans. Power Deliv.*, vol. 35, no. 1, pp. 396–407, Feb. 2020, doi: 10.1109/TPWRD.2019.2920690.

[7] I. Ahmad *et al.*, "Sensitivity analysis of entrained flow coal gasification process through Fourier amplitude sensitivity test (FAST) and Sobol techniques," *2018 Int. Conf. Appl. Eng. Math. (ICAEM)*, 2018, pp. 79–84, doi: 10.1109/ICAEM.2018.8536285.

[8] A. Saltelli, S. Tarantola, F. Campolongo, and M. Ratto, *Sensitivity Analysis in Practice: A Guide to Assessing Scientific Models*. Chichester, England: John Wiley & Sons Ltd, 2004.

[9] Y. Zhou *et al.*, "Candidate bus selection method for VAR planning of wind-penetrated power system based on Morris screening method," *2019 IEEE 3rd Conf. Energy Internet Energy Syst. Integr. (EI2)*, 2019, pp. 2487–2492, doi: 10.1109/EI247390.2019.9061879.

[10] *SEL-421 Relay Protection and Automation System Instruction Manual User's Guide*, Schweitzer Engineering Laboratories, INC, Pullman, WA, USA, 2007.

[11] *User's Manual DIgSILENT PowerFactory Version 14.0*, DIgSILENT GmbH, Gomaringen, Germany, 2008.

[12] A.M. Tsimtsios and V.C. Nikolaidis, "Setting zero-sequence compensation factor in distance relays protecting distribution systems," *IEEE Trans. Power Deliv.*, vol. 33, no. 3, pp. 1236–1246, Jun. 2018, doi: 10.1109/TPWRD.2017.2762465.

[13] M.N. Uddin, N. Rezaei, and M.S. Arifin, "Hybrid machine learning-based intelligent distance protection and control schemes with fault and zonal classification capabilities for grid - Connected wind farms," *IEEE Trans. Ind. Appl.*, vol. 59, no. 6, pp. 7328–7340, Nov./Dec. 2023, doi: 10.1109/TIA.2023.3302836.

[14] H. Junjie *et al.*, "Analysis of the effect of UHV series compensation capacitor on distance protection," *2018 2nd IEEE Conf. Energy Internet Energy Syst. Integr. (EI2)*, 2018, pp. 1–5, doi: 10.1109/EI2.2018.8582587.

[15] S. Wu, Z. Liu, and J. Li, "Global sensitivity analysis based on Inception-CNN," *2020 Chin. Control Decis. Conf. (CCDC)*, 2020, pp. 3818–3823, doi: 10.1109/CCDC49329.2020.9164657.

[16] P. Zhang, Y. Wang, X. Peng, and S. Yang, "An improved screening method based on standard Morris for learning neural network," *2018 13th World Congr. Intell. Control Automat. (WCICA)*, 2018, pp. 88–92, doi: 10.1109/WCICA.2018.8630508.

[17] K. Ye et al., "Global sensitivity analysis of large distribution system with PVs using deep Gaussian process," *IEEE Trans. Power Syst.*, vol. 36, no. 5, pp. 4888–4891, Sep. 2021, doi: 10.1109/TPWRS.2021.3084455.

[18] K. Ye *et al.*, "A data-driven global sensitivity analysis framework for three-phase distribution system with PVs," *IEEE Trans. Power Syst.*, vol. 36, no. 5, pp. 4809–4819, Sep. 2021, doi: 10.1109/TPWRS.2021.3069009.

[19] N. Rohadi and R. Živanović, "Sensitivity analysis of impedance measurement algorithms implemented in intelligent electronic devices," *2022 30th Mediterr. Conf. Control Automat. (MED)*, 2022, pp. 1042–1046, doi: 10.1109/MED54222.2022.9837121.

[20] J. Guo, J. Xiao, S. Liu, and T. Wang, "Research on global uncertainty and sensitivity analysis (SA) algorithms based on the development of energy internet," *2019 IEEE Int. Conf. Energy Internet (ICEI)*, 2019, pp. 86–91, doi: 10.1109/ICEI.2019.00022.

[21] K. He, X. Xu, H. Wang, and Z. Yan, "Global sensitivity analysis of islanded microgrid power flow," *2018 IEEE Power Energy Soc. Gen. Meet. (PESGM)*, 2018, pp. 1–5, doi: 10.1109/PESGM.2018.8586617.